NASA Technical Memorandum 104647

Arctic and Antarctic Sea Ice Concentrations from Multichannel Passive-Microwave Satellite Data Sets: October 1978 – September 1995

User's Guide

Donald J. Cavalieri, Claire L. Parkinson, Per Gloersen, and H. Jay Zwally

National Aeronautics and
Space Administration

Goddard Space Flight Center
Greenbelt, Maryland
1997

NASA Technical Memorandum 104647

Arctic and Antarctic Sea Ice Concentrations from Multichannel Passive-Microwave Satellite Data Sets: October 1978 – September 1995

User's Guide

Donald J. Cavalieri
Claire L. Parkinson
Per Gloersen
H. Jay Zwally
Goddard Space Flight Center
Greenbelt, Maryland

National Aeronautics and
Space Administration

Goddard Space Flight Center
Greenbelt, Maryland
1997

This publication is available from the NASA Center for AeroSpace Information,
800 Elkridge Landing Road, Linthicum Heights, MD 21090-2934, 301-621-0390.

TABLE OF CONTENTS

1.0 Introduction

Satellite multichannel passive-microwave sensors have provided global radiance measurements with which to map, monitor, and study the Arctic and Antarctic polar sea ice covers. The data span over 18 years (as of April 1997), starting with the launch of the Scanning Multichannel Microwave Radiometer (SMMR) on NASA's SeaSat A and Nimbus 7 in 1978 and continuing with the Defense Meteorological Satellite Program (DMSP) Special Sensor Microwave/Imager (SSMI) series beginning in 1987. It is anticipated that the DMSP SSMI series will continue into the 21st century. The SSMI series will be augmented by new, improved sensors to be flown on Japanese and U.S. space platforms.

This User's Guide provides a description of a new sea ice concentration data set generated from observations made by three of these multichannel sensors. The data set includes gridded daily ice concentrations (every-other-day for the SMMR data) for both the north and south polar regions from October 26, 1978 through September 30, 1995 with the one exception of a 6-week data gap from December 3, 1987 through January 12, 1988. The data have been placed on two CD-ROMs that include a ReadMeCD file (Fiegles and Gloersen, 1997) giving the technical details on the file format, file headers, north and south polar grids, ancillary data sets, and directory structure of the CD-ROM.

The goal in the creation of the data set was to produce a long term, consistent set which would serve as a baseline for future measurements. This User's Guide summarizes the problems encountered when working with radiances from sensors having different frequencies, different footprint sizes, different visit times, and different calibrations. A major obstacle to resolving these differences was the lack of sufficient overlapping data from sequential sensors. The techniques we employed to solve these problems or at least reduce their impacts are also presented. In the following sections, we discuss the mapping of the sensor data onto a common grid, the application of a new landmask, instrument drift, adjustment for land-ocean spillover, replacement of bad data, and intersensor corrections made to reduce remaining measurement differences.

2.0 Multichannel Passive-Microwave Satellite Data Sets

The three satellite data sets employed and the periods for which the data are usable are: the Nimbus 7 SMMR from October 26, 1978 through August 20, 1987, the DMSP SSMI F8 from July 9, 1987 through December 18, 1991 (with the exception of the data gap from December 3, 1987 through January 12, 1988), and the DMSP SSMI F11 from December 3, 1991 through September 30, 1995. A single-channel and two other multichannel passive-microwave satellite imagers flown in the 1970s, but not included here, are the Nimbus 5 ESMR, the Nimbus 6 ESMR and the SeaSat SMMR respectively. The Nimbus 5 ESMR was not used because of the lack of overlap data with the Nimbus 7 SMMR, while the Nimbus 6 ESMR was omitted because of the poor quality of the data. The SeaSat SMMR was omitted because of not providing adequate coverage of the polar regions. For the purpose of providing a consistent long-term data set, data from each of the three sensors used were mapped onto the SSMI north and south polar grids (NSIDC, 1992) and a common land mask, recently updated for the SSMI grids (Martino et al., 1995), was applied.

2.1 Nimbus 7 SMMR

Descriptions of the SMMR instrument design, the operating characteristics, and the procedures used to obtain calibrated brightness temperatures and sea ice concentrations are given by Gloersen et al. (1992). The algorithm to obtain sea ice concentration employs three of the ten channels of the SMMR instrument: vertically and horizontally polarized radiances at 18 GHz and vertically polarized radiances at 37 GHz. Before computing sea ice concentrations, isolated missing brightness temperature pixels on the daily brightness temperature maps were filled by spatial interpolation. Larger areas of missing data were filled later by temporal interpolation of the sea ice concentrations.

Gloersen et al. (1992) also describe the corrections used for a long-term drift in the SMMR data and for errors related to ecliptic-angle that were observed in the 8.8-year data set. These and other errors had been accommodated in the sea ice concentration data set used in the Gloersen et al. (1992) monthly averages without also correcting the gridded radiances. Since the publication of Gloersen et al. (1992), some additional errors have been identified in the gridded brightness temperature data set. The nature of these errors fall into four categories. These are: full orbits of bad data, individual scans of bad data, misplaced scans from the opposite node, and misplaced scans from unknown origin. These were identified by checking each daily image from both the ascending node data and the descending node data. All of the errors identified and considered to be sufficiently serious to warrant exclusion were removed in the ascending and descending node data sets separately before averaging the data from the two nodes to provide daily brightness temperature matrices. Finally, additional corrections were applied to the three channels (18 GHz H & V, 37 GHz V) of previously corrected data used in the sea ice algorithm (Gloersen et al., 1992), following a procedure similar to that described in Gloersen et al. (1992), but with higher precision. The 8.8-year drifts in these channels were reduced to values well below the instrument noise values given in Gloersen and Barath (1977) and lower than in the previously corrected data.

2.2 DMSP F8 and F11 SSMI

The DMSP F8 and F11 SSMI data were obtained from the National Snow and Ice Data Center (NSIDC) in Boulder, Colorado. The F8 data were distributed by NSIDC on CD-ROMs for the period July 1987 through December 1991 and the F11 data for the period December 1991 through September 1995. Data acquisition, filtering bad data, handling geolocation errors, implementation of an antenna pattern correction, and finally the swath-to-grid conversion are all described in the NSIDC's User's Guide (1992).

The 4.5-year F8 19-37 GHz data were found to be free of orbit-dependent (ecliptic angle) brightness temperature variations using a technique similar to what was used for the SMMR data (Gloersen et al., 1992). At the time of the analysis, the F11 data set was too short to warrant a similar analysis, but based on the F8 experience, the F11 SSMI was presumed also to be free of this defect. The drift determined by the method used for the SMMR data over the 7-year SSMI period resulted in brightness temperature changes below or at the instrument noise level for the SSMI (see Table 1.4 in Hollinger, 1989), and was therefore considered to have no significant impact on the computed sea ice concentrations (less than 0.5%) either for consolidated sea ice or at the ice edge, and so were ignored.

3.0 Data Processing

3.1 Calculation of Sea Ice Concentrations

Comparisons of sea ice concentrations calculated for each of the sensors during overlap periods using published algorithm tie-points reveal significant differences. These differences may result from differences in sensor and orbital characteristics, differences in observation times (and therefore tidal effects), and differences in algorithm coefficients. Sensor and orbital characteristic differences for the Nimbus 7 SMMR and DMSP SSMI F8 include antenna beam width, channel frequency, spacecraft altitude, ascending node time, and angle of incidence. In addition, the sea ice algorithm tie-points are significantly different. The SSMI F8 and F11 sensors also differ in ascending node time, altitude, and angle of incidence. Because the visit times of the three satellites occur during different phases of the diurnal cycle, tidal effects may result in differences in the ice distribution. We are presuming that any such effects are mitigated by the correction scheme described below. Table 1 summarizes the sensor and orbital characteristic differences. These differences are accommodated for each pair of sensors by employing a self-consistent set of algorithm tie-points determined through linear relationships between the observed brightness temperatures during the overlap periods.

Nimbus 7 SMMR/DMSP SSMI F8

Daily brightness temperature maps from the Nimbus 7 SMMR and from the DMSP SSMI F8 during their period of overlap, July 9–August 20, 1987, were compared for both the Arctic and Antarctic. Unfortunately, there were only 22 days of common coverage. A linear least squares best fit of the cumulative data was obtained for each of the corresponding channels. For the purpose of eliminating spurious brightness temperatures resulting from residual land spillover effects, an Arctic land mask expanded 3 to 4 pixels out from the original land mask was used in the determination of the best fit between the two data sets. The eliminated pixels represent only a very small fraction of the total number of ice concentration pixels, but eliminating them helps considerably in reducing the outliers on the scatter plots. The linear regression equations obtained and the standard error of estimates for the corresponding channels are given in Table 2. These linear relationships were used to generate a set of SSMI tie-points that are consistent with the original SMMR sea ice algorithm tie-points (Gloersen et al., 1992). The published SSMI F8 tie-points (Cavalieri et al., 1992) were not used. In addition to using these transformations, the SSMI F8 open water tie-points were subjectively tuned to help minimize the differences between the SMMR and SSMI F8 sea ice extent and area during the overlap period. The SMMR set of tie-points, the tuned SSMI F8 set, and the resulting percent differences in ice extent and area given during the period of overlap are given in Table 3. The amount of tuning is also indicated for the open water tie-points. In all cases except for the Antarctic F8 values, the tuned amount is within one standard error of estimate. We suspect the reason for the larger tuned values results from greater weather effects during the overlap period.

SSMI F8/SSMI F11

The period of overlap for F8 and F11 is even shorter than that for Nimbus 7 and SSMI F8, with only 16 days of overlap of good data, from December 3-18, 1991. The linear regression equations obtained from these plots and the standard error of estimates for the corresponding channels are given in Table 2. The SSMI F11 open water tie-points were also tuned to help reduce differences in ice extent and area as was done with the SSMI F8 values. A further adjustment to the Antarctic 37V ice type-B F11 tie-point was also made to reduce the ice area difference. The tie-points, the amount of tuning, the ice extent and area percent differences are all given in Table 3. In this case, the amount of tuning needed to reduce the ice extent and area differences between the F8 and F11 values is well within one standard error of estimate (Table 2).

3.2 Land-to-Ocean Spillover and Residual Weather-Related Effects

The next step in preparing the data sets was the correction for land-to-ocean spillover (often referred to as "land contamination") and residual weather-related effects. Land-to-ocean spillover refers to the problem of blurring sharp contrasts in brightness temperature, such as exist between land and ocean, by the relatively coarse width of the sensor antenna pattern (Figure 1a). This problem is of concern here because it results in false sea ice signals along coastlines. The method used to reduce the spillover is an extension of the method employed for the single-channel Nimbus 5 Electrically Scanning Microwave Radiometer (ESMR) data in Parkinson et al. (1987). The rationale behind the approach is that a minimum observed (generally in late summer) sea ice concentration in the vicinity of coastlines where no ice remains offshore is probably the result of land spillover and is thus subtracted from the image. To reduce the error of subtracting ice in areas of ice cover, the technique searches for and requires the presence of open water in the vicinity of the image pixel to be corrected.

Land-to-ocean spillover was reduced by the following three-step procedure:

(1) A matrix M was created covering the entire grid and identifying each pixel as land, shore, near-shore, off-shore, or non-coastal ocean. The identification of land pixels was straightforward, obtained from the land/sea mask. The identification of shore, near-shore, and off-shore pixels was based on the scheme plotted in Figure 1b, where the pixel to be identified is labeled I,J. This pixel is considered a "shore" pixel if any pixel adjacent to it (the A pixels in Figure 1b) is land, a "near-shore" pixel if none of the A pixels is land but at least one of the B pixels is land,

and an "off-shore" pixel if none of the A or B pixels is land but at least one of the C pixels is land. All other ocean pixels are considered "non-coastal ocean". This matrix M is created once and then used throughout the data set.

(2) A matrix CMIN, to represent minimum ice concentrations on a pixel-by-pixel basis throughout the entire grid, was created for each instrument type. CMIN was created by first constructing a matrix P containing the minimum monthly average ice concentrations throughout a given year, then adjusting that matrix at off-shore, near-shore, and shore pixels. In the case of SMMR, 1984 monthly data were used, whereas in the case of SSMI, 1992 monthly data were used. In both cases, the adjustments were as follows: (a) at off-shore pixels, any P values exceeding 20% were reduced to 20%; (b) at near-shore pixels, any P values exceeding 40% were reduced to 40%; and (c) at shore pixels, any P values exceeding 60% were reduced to 60%. The CMIN matrix was created once for SMMR and once for SSMI, then used throughout the data sets.

(3) The daily ice-concentration matrices for all three data sets were adjusted at any off-shore, near-shore, and shore pixels in the vicinity of open water. Specifically, the "neighborhood" of an off-shore pixel was defined as containing the 8 other pixels in the 3 x 3 box centered on the off-shore pixel; the "neighborhood" of a near-shore pixel was defined as containing the 24 other pixels in the 5 x 5 box centered on the near-shore pixel; and the "neighborhood" of a shore pixel was defined as containing the 48 other pixels in the 7 x 7 box centered on the shore pixel. At any time when the neighborhood of an off-shore, near-shore, or shore pixel contains three or more open-water pixels (i.e., ice concentration less than 15%), then the calculated ice concentration at the off-shore, near-shore, or shore pixel is reduced by the value for that pixel in the matrix CMIN. Wherever the subtraction leads to negative ice concentrations, the concentrations are set to 0%. This land-spillover-correction algorithm is clearly a rough approximation, as the contaminated amount does not stay constant over time; but the scheme has been found to reduce substantially the spurious ice concentrations on the grids.

A correction for residual weather effects was made based on monthly climatological sea surface temperatures (SSTs) from the NOAA Ocean Atlas (Levitus and Boyer, 1994). These data, originally on a 2° by 2° grid, were remapped onto the SSMI grid. Because the SST data did not extend to the SSMI coastline, the data were extrapolated to the coastline once regridded onto the SSMI grid. The SST maps were used as follows: In the Northern Hemisphere, in any pixel where the monthly SST is greater than 278 K, the ice concentration is set to zero throughout the month; in the Southern Hemisphere, wherever the monthly SST is greater than 275 K, the ice concentration is set to zero throughout the month. The higher threshold SST value was needed in the Northern Hemisphere because the 275 K isotherm used in the South was too close to the ice edge in the North. In a few instances, corrections to the regridded SST data were needed, because otherwise we were losing actual sea ice. An example of the application of the land-ocean spillover and residual weather effect corrections is provided in Figure 2.

3.3 Filling Data Gaps

In each of the data sets, there are instances of missing data. In some cases whole days (or weeks or months) are missing. In other cases, large swaths or wedges of missing data exist within an image, along with scattered pixels of missing data throughout the grid. The scattered pixels of missing data, resulting generally from mapping the orbital radiance data to the SSMI grid, were filled by applying a spatial linear interpolation scheme on the brightness temperature maps. The larger areas of missing data, resulting from gaps between orbital swaths (generally at low latitudes on daily maps) or from partial coverage or missing days, were filled by temporal interpolation on the ice concentration maps. No data at all were available for the period from December 2, 1987 through January 12, 1988. This gap was not filled by temporal linear interpolation, instead being left as missing data. Table 4 lists the SSMI dates containing bad data, which were subsequently corrected through interpolation.

♦ ♦♦

Acknowledgments

We gratefully acknowledge the help of S. Fiegles, M. Martino, and J. Saleh from Hughes STX Corp. with various aspects of this project. The SSMI data were obtained on CD-ROM from the National Snow and Ice Data Center, Boulder, CO.

4.0 References

Cavalieri, D. J., J. Crawford, M. Drinkwater, W. J. Emery, D. T. Eppler, L. D. Farmer, M. Goodberlet, R. Jentz, A. Milman, C. Morris, R. Onstott, A. Schweiger, R. Shuchman, K. Steffen, C. T. Swift, C. Wackerman and R. L. Weaver, *NASA Sea Ice Validation Program for the DMSP SSM/I: Final Report*, *NASA Technical Memorandum 104559*, National Aeronautics and Space Administration, Washington, D. C., pp. 126, 1992.

Fiegles, S. and P. Gloersen, “README file on CDROM,” *Arctic Sea Ice: 1978-1995*, National Aeronautics and Space Administration, Washington, D.C., 1997.

Gloersen, P., W. J. Campbell, D. J. Cavalieri, J. C. Comiso, C. L. Parkinson, H. J. Zwally, *Arctic and Antarctic Sea Ice,1978-1987: Satellite Passive Microwave Observations and Analysis*, National Aeronautics and Space Administration, *Special Publication 511*, Wash ington, D.C., pp.290, 1992.

Gloersen, P. and Barath, F. T., “A Scanning Multichannel Microwave Radiometer for Nimbus-G and SeaSat-A,” *IEEE Journal of Oceanic Engineering, OE-2*, 172-178, 1977.

Hollinger, J. P., *DMSP Special Sensor Microwave/Imager Calibration/Validation, Final Report Volume 1*, Space Sensing Branch, Naval Research Laboratory, Washington, DC 20375-5000, 20 July 1989.

Levitus, S. and Boyer, T. P., *World Ocean Atlas 1994, Volume 4: Temperature*, NOAA National Oceanographic Data Center, Ocean Climate Laboratory, U.S. Department of Commerce, Washington, D.C., 1994.

Martino, M., D. J. Cavalieri, P. Gloersen, and H. J. Zwally, *An Improved Land Mask for the SSM/I Grid, NASA Technical Memorandum 104625*, pp.9, December 1995.

NSIDC, DMSP SSM/I Brightness Temperatures and Sea Ice Concentration Grids for the Polar Regions on CD-ROM User’s Guide, National Snow and Ice Data Center, Special Report-1, Cooperative Institute for Research in Environmental Sciences, University of Colorado, Boulder, CO, January 1992.

Parkinson, C. L., J. Comiso, H. J. Zwally, D. J. Cavalieri, P. Gloersen, W. J. Campbell, *Arctic Sea Ice, 1973-1976: Satellite Passive Microwave Observations*, National Aeronautics and Space Administration, *Special Publication 489*, Washington, D.C., 296 pp., 1987.

5.0 Tables and Figures

Table 1. Sensor and spacecraft orbital characteristics of the three sensors used in generating the sea ice concentrations.

CHARACTERISTIC	SENSOR		
	Nimbus 7 SMMR	DMSP SSMI F8	DMSP SSMI F11
Nominal Altitude (km)	955	860	830
Equatorial Crossing of Ascending Node (approx. local time)	1200	0600	1700
Algorithm Frequencies (GHz)	18.0 & 37.0	19.4 & 37.0	19.4 & 37.0
3 dB Beam Width (degree)	1.6, 0.8	1.9, 1.1	1.9, 1.1
Earth Incidence Angle	50.2	53.1	52.8

Table 2. Brightness temperature linear regression coefficients and standard errors of estimates for each sensor pair during their respective periods of overlap.

			Slope	Intercept	Std.Err.
Arctic	X(SMMR)	Y(SSMI/F8)			
	18v	19v	0.919267	28.8415	3.3
	18h	19h	0.963816	18.4413	5.5
	37v	37v	0.979575	7.07773	3.8
Antarctic	X(SMMR)	Y(SSMI/F8)			
	18v	19v	0.957788	19.9111	3.5
	18h	19h	0.997198	11.0883	6.0
	37v	37v	1.00475	1.40737	3.7
Arctic	X(SSMI/F8)	Y(SSMI/F11)			
	19v	19v	0.980904	4.70857	2.5
	19h	19h	0.999773	-0.0962	4.6
	37v	37v	0.983745	3.91561	2.8
Antarctic	X(SSMI/F8)	Y(SSMI/F11)			
	19v	19v	0.967175	7.37425	2.8
	19h	19h	0.988334	1.38727	4.9
	37v	37v	0.905892	20.8818	4.3

where Std. Err. = rms($Y-Y_{est}$)

Table 3. New Sensor Tie-Points Used to Reduce Sea Ice Extent and Area Differences Between Sensors During Their Respective Overlap Periods

			NIMBUS 7 SMMR						
ARCTIC		18H		18V		37V			
	OW	98.5		168.7		199.4			
	FY	225.2		242.2		239.8			
	MY	186.8		210.2		180.8			
ANTARCTIC									
	OW	98.5		168.7		199.4			
	A	232.2		247.1		245.5			
	B	205.2		237.0		210.0			
			DMSP SSMI F8					%DIFF.(F8-N7)	
ARCTIC		19H	Δ	19V	Δ	37V	Δ	ΔIE	ΔIA
	OW	113.2	+0.2	183.4	+0.5	204.0	-1.6	+0.0069	-0.41
	FY	235.5		251.5		242.0			
	MY	198.5		222.1		184.2			
ANTARCTIC									
	OW	117.0	+7.7	185.3	+3.8	207.1	+5.3	+0.019	-0.11
	A	242.6		256.6		248.1			
	B	215.7		246.9		212.4			
			DMSP SSMI F11					%DIFF.(F11-F8)	
ARCTIC		19H	Δ	19V	Δ	37V	Δ	ΔIE	ΔIA
	OW	113.6	+0.5	185.1	+0.5	204.8	+0.2	+0.0048	+0.21
	FY	235.3		251.4		242.0			
	MY	198.3		222.5		185.1			
ANTARCTIC									
	OW	115.7	+0.1	186.2	-0.4	207.1	-1.4	-0.036	+0.61
	A	241.2		255.5		245.6			
	B	214.6		246.2		211.3	-2.0		

Table 4. SSMI (F8 and F11) days containing bad orbits or bad scans.

Dates				
102/1992	103/1992	351/1992	323/1993	330/1993
331/1993	334/1993	346/1993	352/1993	357/1993
007/1994	009/1994	011/1994	012/1994	014/1994
017/1994	019/1994	022/1994	023/1994	025/1994
028/1994	031/1994	042/1994	167/1994	182/1994
350/1994	358/1994	003/1995	039/1995	059/1995
077/1995	081/1995	082/1995	086/1995	097/1995
105/1995	231/1995	232/1995		

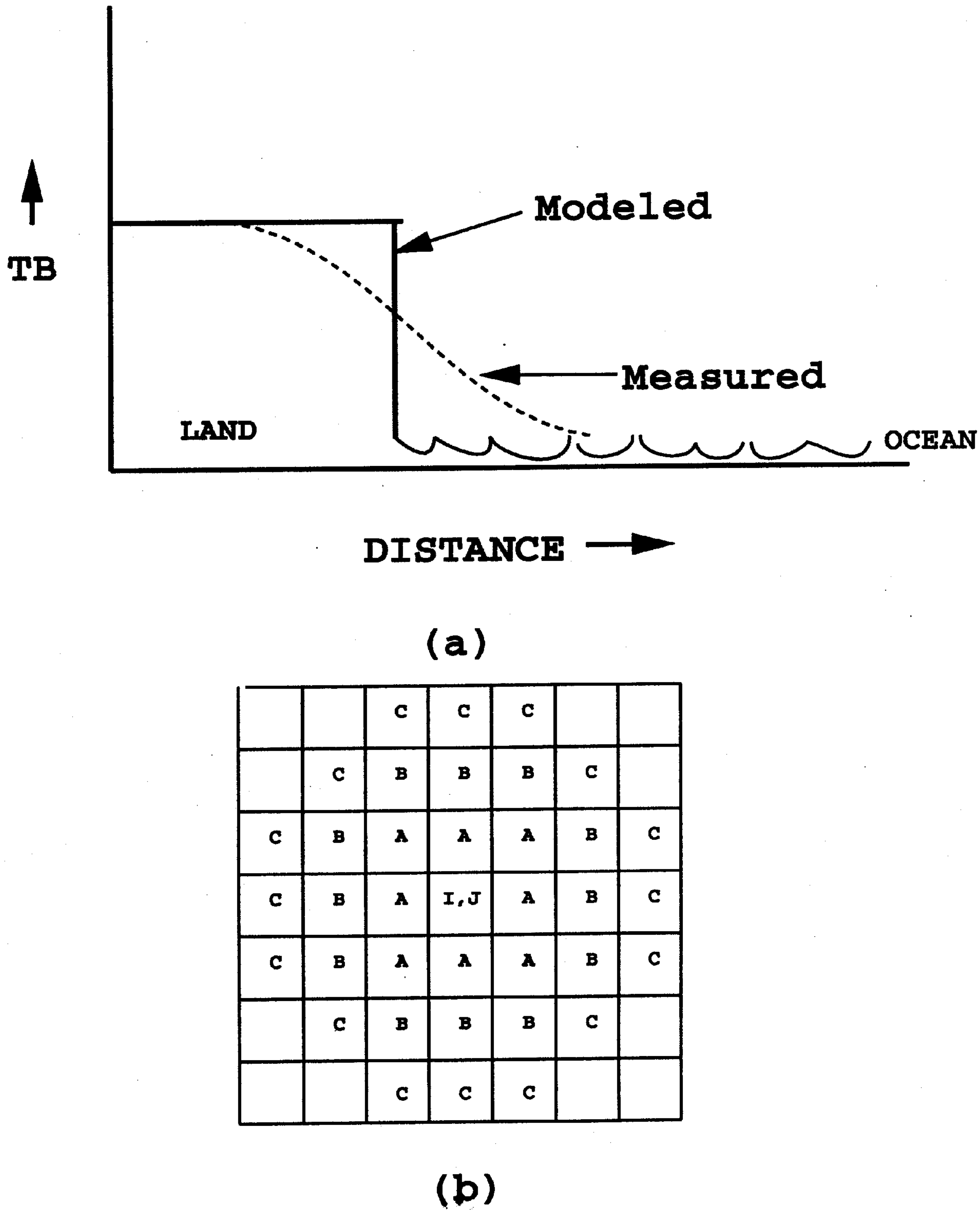

Figure 1. (a) Schematic illustrating the effect of the coarse resolution of the microwave antenna on a coastline. This effect, referred to as land-to-ocean spillover, results in false sea ice signals in the vicinity of the coast. (b) Seven-by-seven array used in the procedure to reduce the land-to-ocean spillover effect. See text for explanation.

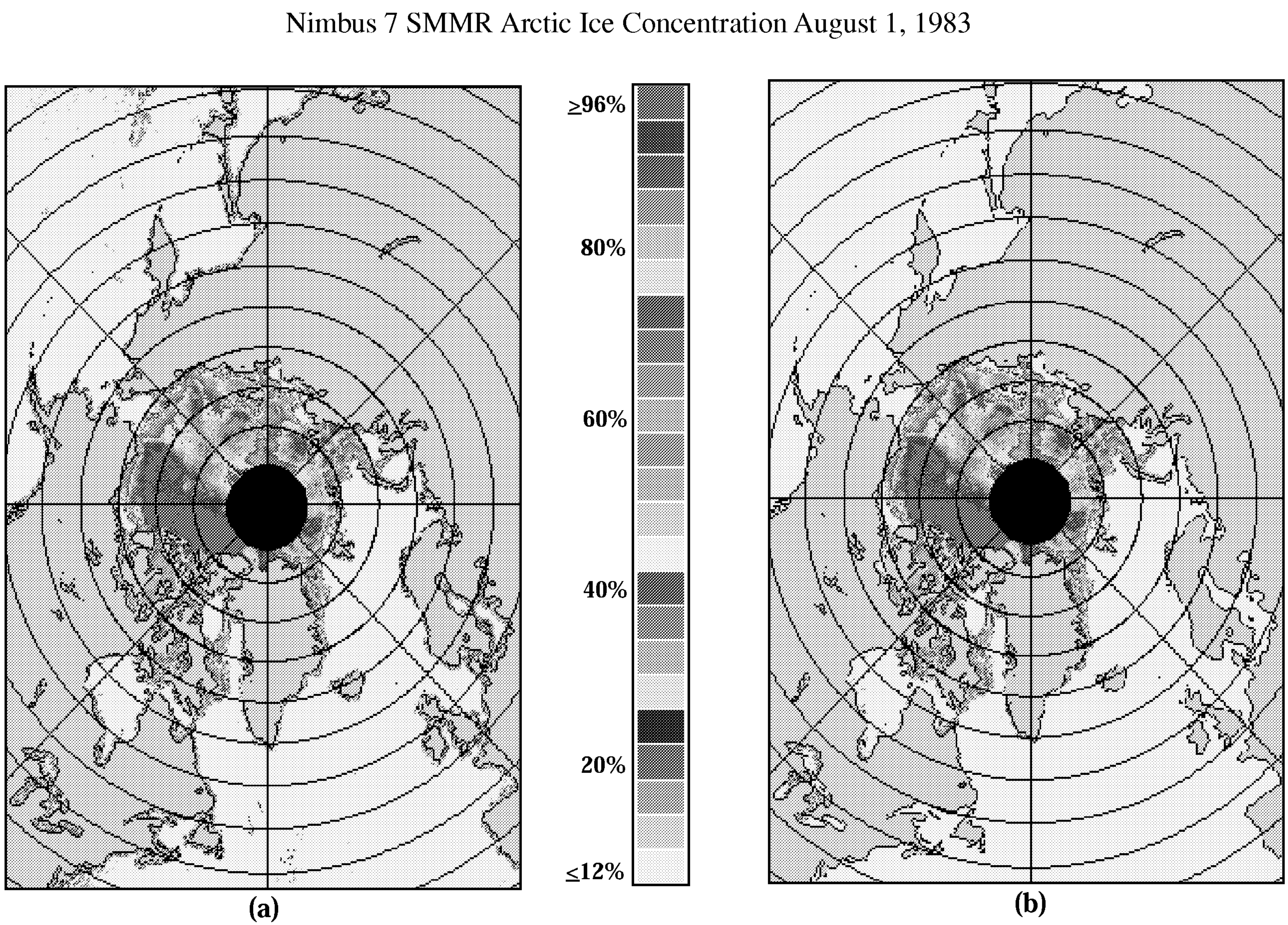

Figure 2. Nimbus 7 SMMR sea ice concentration map of the Arctic for August 1, 1983 (a) before and (b) after the application of the land spillover and residual weather corrections.

REPORT DOCUMENTATION PAGE

Form Approved
OMB No. 0704-0188

1. AGENCY USE ONLY *(Leave blank)*	2. REPORT DATE	3. REPORT TYPE AND DATES COVERED
	May 1997	Technical Memorandum

4. TITLE AND SUBTITLE

Arctic and Antarctic Sea Ice Concentrations from Multichannel Passive-Microwave Satellite Data Sets: Oct. 1978 - Sept. 1995

5. FUNDING NUMBERS

Code 971

6. AUTHOR(S)

D. J. Cavalieri, C. L. Parkinson, P. Gloersen, and H. Jay Zwally

7. PERFORMING ORGANIZATION NAME(S) AND ADDRESS (ES)

Laboratory for Hydrospheric Processes
Goddard Space Flight Center
Greenbelt, Maryland 20771

8. PEFORMING ORGANIZATION REPORT NUMBER

97B00054

9. SPONSORING / MONITORING AGENCY NAME(S) AND ADDRESS (ES)

National Aeronautics and Space Administration
Washington, DC 20546-0001

10. SPONSORING / MONITORING AGENCY REPORT NUMBER

TM-104647

11. SUPPLEMENTARY NOTES

12a. DISTRIBUTION / AVAILABILITY STATEMENT

Unclassified - Unlimited
Subject Category: 43
This report is available from the NASA Center for AeroSpace Information, 800 Elkridge Landing Road, Linthicum Heights, MD 21090;301-621-0390

12b. DISTRIBUTION CODE

13. ABSTRACT *(Maximum 200 words)*

Satellite multichannel passive-microwave sensors have provided global radiance measurements with which to map, monitor and study the Arctic and Antarctic polar sea ice covers. The data span over 18 years (as of April 1997), starting with the launch of the Scanning Multichannel Microwave Radiometer (SMMR) on NASA's SeaSat A and Nimbus 7 in 1978 and continuing with the Defense Meteorological Satellite Program (DMSP) Special Sensor Microwave/Imager (SSMI) series beginning in 1987. It is anticipated that the DMSP SSMI series will continue into the 21st century. The SSMI series will be augmented by new, improved sensors to be flown on Japanese and U.S. space platforms.

This User's Guide provides a description of a new sea ice concentration data set generated from observations made by three of these multichannel sensors. The data set includes gridded daily ice concentrations (every-other-day for the SMMR data) for both the north and south polar regions from October 26, 1978 through September 30, 1995, with the one exception of a 6-week data gap from December 3, 1987 through January 12, 1988. The data have been placed on two CD-ROMs that include a ReadMeCD file giving the technical details on the file format, file headers, north and south polar grids, ancillary data sets, and directory structure of the CD-ROM. The CD-ROMS will be distributed by the National Snow and Ice Data Center in Boulder, CO.

14. SUBJECT TERMS

sea ice concentration, satellite passive microwave radiometers, Arctic sea ice, Antarctic sea ice

15. NUMBER OF PAGES

17

16. PRICE CODE

17. SECURITY CLASSIFICATION OF REPORT	18. SECURITY CLASSIFICATION OF THIS PAGE	19. SECURITY CLASSIFICATION OF ABSTRACT	20. LIMITATION OF ABSTRACT
Unclassified	Unclassified	Unclassified	UL